N O T I C E

Adhesion and Friction of Transition Metals in Contact with Nonmetallic Hard Materials

Kazuhisa Miyoshi and Donald H. Buckley
Lewis Research Center
Cleveland, Ohio

NASA

ADHESION AND FRICTION OF TRANSITION METALS

IN CONTACT WITH NONMETALLIC HARD MATERIALS

Kazuhisa Miyoshi and Donald H. Buckley

National Aeronautics and Space Administration
Lewis Research Center
Cleveland, Ohio

INTRODUCTION

A phenomenon incidental to the interaction of two solid sur-
faces most commonly observed is friction. Friction usually in-
cludes adhesion of the two solid surfaces in contact.

In order to gain a fundamental understanding of the surface
interactions between metals and nonmetals, it is extremely impor-
tant to consider the basic material properties that determine and
influence adhesion and friction.

The authors have studied surface interactions for many years
and have been interested in fundamental experimental studies to
determine the basic material properties of metals that relate to
the adhesion and friction of metals in sliding contact with nonme-
tallic hard materials, such as diamond, silicon carbide, boron
nitride and manganese-zinc ferrite (refs. 1 to 4).

Diamond, the hardest known material, is generally used for
machining nonferrous alloys, abrasive materials (such as presin-
tered carbide, borides and nitrides), graphite, fiberglass and
rubber. Diamond is also widely used in the electronics and jew-
elry industries as a wear resistant coating material and in ma-
chining tools as well.

Silicon carbide has been used and has great potential for use
in high-hardness and high temperature applications such as stable
high-temperature semiconductors, turbine ceramic seal systems, gas
turbine blades and as an abrasive in grinding.

Boron nitride would be a good solid lubricant if it's adhesion to metals could be improved. This has, however, not been achieved to date.

Manganese-zinc ferrite is very important as a typical magnetic material used for highly developed magnetic recording devices, that is, video tape recorders. It is therefore widely used.

Most of the foregoing applications of hard nonmetallic materials deeply involve surface interactions. Understanding surface interactions and reactions is therefore important.

In the 1940's Pauling recognized differences in the amount of a d-bond character associated with transition metals. The filling of d-electron band he found to be responsible for various physical and chemical properties including adhesive energy, Young's and shear moduli, tensile and shear strengths, chemical stability, and magnetic properties (ref. 5). The greater the amount or percentage of d-bond character that a metal possesses, the less active is its surface.

The effect of the chemical properties of metals on adhesion and friction should be identified. The knowledge gained in such studies will assist in achieving a better understanding of the adhesion and friction properties of metals sliding against nonmetals.

The objective of this paper is to discuss the adhesion and friction properties of various transition metals in contact with various nonmetallic hard materials. The transition metals examined include yttrium, titanium, tantalum, zirconium, vanadium, neodymium, iron, cobalt, nickel, tungsten, platinum, rhenium, ruthenium, and rhodium. The nonmetals examined were single-crystal diamond, silicon carbide, boron nitride and manganese-zinc ferrite. The investigation also examined metal transfer to the hard nonmetallic materials. All the experiments were conducted with a metal pin contacting a nonmetallic hard material flat at loads of 0.05 to 0.3 N, at a sliding velocity of 3 or 0.7×10^{-3} m/min, in a vacuum of 10^{-8} Pa at room temperature. The radius of the metal pin specimens was 0.79 mm.

MATERIALS

The metals were in both polycrystalline and single-crystal forms. The polycrystalline metals were used for the experiments with diamond, silicon carbide and manganese-zinc ferrite. The single-crystal metals were used for those studies with pyrolytic boron nitride. The titanium was 99.97 percent pure; the yttrium

was 99.9 percent pure; the vanadium was 99.95 percent pure; and all the other metals were 99.99 percent in purity. For the single crystals, the body centered cubic metals had the {110} plane on their surface and, therefore, parallel to the sliding surface. The face centered cubic metals had the {111} planes parallel to the sliding interface and the hexagonal metals had the {0001} surfaces parallel to that interface.

Natural, single-crystal diamonds were used in these experiments. The {111} plane was parallel to the sliding interface (ref. 1).

The single-crystal silicon carbide used in these experiments was a 99.9 percent pure compound of silicon and carbon. Silicon carbide has a hexagonal close-packed crystal structure. The basal plane was parallel to the interface (ref. 2).

The pyrolytic boron nitride employed in these experiments was a 99.99 percent pure compound of boron and nitrogen (ref. 3). It has a hexagonal crystal structure, and the basal plane was parallel to the interface.

The single-crystal manganese-zinc ferrite was 99.9 percent pure oxide (ref. 4) The crystal is that of a spinel structure in which the oxygen ions are in a nearly closed-packed cubic array. The {110} plane was parallel to the sliding interface.

All the nonmetal specimens used herein were within +2° of the designated plane. All the specimens of nonmetals were in the form of flat platelets.

APPARATUS

An Ultra-High Vacuum system was used in this investigation. An apparatus capable of measuring adhesion, load, and friction was mounted in the vacuum system, which also contained a tool for surface analysis, an Auger electron spectrometer (AES). The mechanism used for measuring adhesion, load, and friction is shown schematically in figure 1. A gimbal-mounted beam is projected into the vacuum system. The beam contains two flats machined normal to each other with strain gages mounted on each flat. The metal pin is mounted on the end of the beam. As a load is applied by moving the beam normal to the disk, it is measured by the strain gage.

The vertical sliding motion of the pin along the flat surface is accomplished through a motorized gimbal assembly. Under an applied load the friction force is measured during vertical trans-

lation by the strain gage mounted normal to that used to measure load. This feature was used to examine the coefficient of friction at various loads.

EXPERIMENTAL PROCEDURE

The flat (nonmetallic hard material) and metal pin specimens were cleaned and polished with an aluminum oxide powder (1 μm). The radius of the pins was 0.79 mm. The flat and pin surfaces were rinsed with 200-proof ethyl alcohol.

The specimens were placed in the vacuum chamber, and the system was evacuated and baked out to a pressure of 10^{-8} Pa. Argon gas was then bled back into the vacuum chamber to a pressure of approximately 7×10^{-4} Pa in the case of diamond, and 1.3 Pa in the cases of silicon carbide, boron nitride and ferrite. Then the flat specimen was argon-ion bombarded for 30 to 60 minutes The pin specimens were argon sputter bombarded for 30 minutes at a -1000 V direct-current potential at a vacuum chamber pressure of 1.3 Pa. After the bombardment operation, the vacuum chamber was reevacuated, and AES spectra of the flat surface were obtained to determine the degree of surface cleanliness. When the desired degree of cleanliness of the flat was achieved, friction experiments were conducted.

Loads of 0.05 to 0.3 N were applied to the pin-flat contact by deflecting the beam of figure 1. Both the load and friction force were continuously monitored during friction experiments. Sliding velocity was 3 or 0.7×10^{-3} m/min. All friction experiments were conducted with the system evacuated to a pressure of 10^{-8} Pa.

RESULTS AND DISCUSSION

Surface Cleanliness of Nonmetals

The Diamond Surface – It is extremely difficult to expose {111} diamond faces by cleavage in the vacuum chamber for study in situ, and no entirely satisfactory cleaning procedure has yet been established for diamond. It has been suggested by Lurie and Wilson, on the basis of Auger electron spectroscopic and electron energy loss measurements, that, when diamonds are bombarded with argon ions, their surfaces become graphitized; Thomas and Evans, however, had considered that this treatment merely cleaned the surface (refs. 6 and 7). If Lurie and Wilson's conclusion is correct, surface graphitization of diamond would profoundly influence the tribological properties of the ion-bombarded diamond surface.

The main features in the vicinity of the carbon peaks of the Auger spectra from diamond are shown in figure 2. An Auger electron spectroscopy spectrum of a single-crystal diamond {111} plane obtained before argon-ion bombardment is shown in figure 2(a).

The crystal was in the as-received state after it had been baked out in the vacuum system. A carbon contamination peak is evident, and the spectrum is similar to that of amorphous-carbon. The surface was next argon-ion bombarded at a 3-kilovolt potential, under a pressure of approximately $7x10^{-4}$ Pa for 15, 30, 45, and 60 minutes.

The spectrum of the surface after 15-minutes has three peaks, which are characteristic of graphite. The spectra of the surface after 30, 45, and 60 minutes have four peaks, which are characteristic of diamond, as has been demonstrated and indicated in reference 8.

The peaks have been labelled A_0 to A_3, where A is used to denote an Auger peak. The energy of the peaks in this experiment were 267 to 269 for A_0, 252 to 254 for A_1, 240 eV for A_2, and 230 to 232 eV for A_3. The Auger spectrum of figure 2(d) is essentially the same as that obtained by Lurie for a clean surface (ref. 8). Figure 3 shows the spectrum of a diamond surface after ion bombardment for 60 minutes. A very small sulphur peak is observed in the diamond spectra.

Thus, for the adhesion and friction experiments reported herein, the surfaces of the diamond were argon-ion bombardment for 45 to 60 minutes under the pressure of approximately $7x10^{-4}$ Pa, and the Auger spectra of the surfaces were very similar to that shown in figure 2(d).

The Silicon Carbide Surfaces - An AES spectrum of the single-crystal silicon carbide surfaces obtained before sputter cleaning, but after polishing and bake out, revealed an oxygen peak in addition to the silicon and carbon. The oxygen peak and the chemically shifted silicon peaks at 78 and 89 eV indicated a layer of SiO_2 on the silicon carbide surface as well as a simple, adsorbed film of oxygen. The carbon peak was similar to that obtained for amorphous-carbon (ref. 9). Thus, the spectrum indicated a carbon containment on the silicon carbide surface as well as the SiO_2 layer.

The AES spectrum taken after the silicon carbide surface had been argon-sputter cleaned clearly reveals the silicon at 91 or 92 eV and carbon peaks at 272 eV, as shown in figure 4(a). The carbon peak is of the carbide type, which is characterized by three

peaks labelled A_0 to A_2 in figure 4(a). A small argon peak is evident in the spectrum, but the oxygen peak is negligible.

The Boron Nitride Surface - An Auger electron spectroscopy spectrum obtained from the surface before sputter cleaning revealed that, in addition to the boron and nitrogen peaks, there was a peak adjacent to the boron peaks as well as another peak adjacent to a carbon contamination peak. Oxygen was absent from the surface. An Auger electron spectroscopy spectrum obtained after sputter cleaning is presented in figure 4(b). Sputter cleaning of the boron nitride surface resulted in elimination of contaminant peaks such as sulfur.

The Manganese-Zinc Ferrite Surfaces - An Auger spectra of the as-received single-crystal manganese-zinc ferrite surface obtained before sputter cleaning revealed that, in addition to the oxygen and iron, a carbon contamination peak was evident. An Auger spectrum for ferrite {110} surface after sputter cleaning is shown in figure 4(c). The carbon contamination peak has completely disappeared from the spectrum. In addition to oxygen and iron, the Auger peaks indicate small amounts of manganese and zinc on the surface.

Adhesion and Friction

The removal of adsorbed films (usually water vapor, carbon monoxide, carbon dioxide and oxide layers) from surfaces of metals and nonmetals results in very strong interfacial adhesion when two such solids are brought into contact. For example, when a clean titanium surface is brought into contact with a clean silicon carbide surface, the adhesive bonds formed at the solid-to-solid interface are sufficiently strong that fracture of the cohesive bonds in the metal and transfer of the metal to the silicon carbide surface results. This is indicated in the scanning electron micrograph presented in figure 5.

In figure 5 the light area of the figure, where a lot of metal transfer is evident, was the contact area before and during sliding of the rider. These are the areas where the surfaces of the metal and silicon carbide were sticking, one to the other and where strong interfacial adhesion occurred.

The friction-force traces obtained in this investigation are generally characterized by a marked stick-slip behavior. This type of friction trace clearly indicates that strong adhesion has occurred at the interface. All metals, discussed in this paper, transferred to the cohesively stronger nonmetals.

Effect of Metal Activity on Friction

The data in figure 6 indicates the coefficients of friction for some of the transition metals in contact with a single-crystal diamond {111} surface as a function of the d-bond character of the metal. The percentage of d-bond character can be related to the chemical affinity of the surfaces. The greater the percentage of d-bond character that the metal possesses, the less active its surface should be. The data indicates a decrease in friction with an increase in d-bond character. Titanium and zirconium, which are chemically very active, when in contact with diamond, exhibit very strong interfacial adhesive bonding to diamond. In contrast, rhodium and rhenium, which have a very high percentage of d-bond character have relatively low coefficients of friction.

Figure 6 also presents the friction data for a diamond surface in sliding contact with a yttrium surface. Yttrium gives a higher coefficient of friction than that estimated from data of other metals. This may be due to the effect of oxygen. An argon-sputter-cleaned yttrium surface was covered by an oxide surface layer as shown in figure 7. It is very difficult to remove the oxide surface layer from yttrium by argon-sputter cleaning. The effects of oxygen in increasing the friction is related to the relative chemical thermodynamic properties and bonding of carbon to oxygen. The greater the degree of bonding across the interface, the higher the coefficient of friction. In the case of yttrium, oxygen on the surface tends to strongly chemically bond the yttrium to the diamond surface (ref. 10).

Adhesion and friction properties of the transition metals sliding on other nonmetals, such as silicon carbide, boron nitride and manganese-zinc ferrite are the same as observed for the metals in sliding contact with diamond, as shown in figure 8. The data of figure 8 indicate a decrease in friction with an increase in d character of the metallic bond. In other words, the more active the metal, the higher the coefficient of friction. There appears to be very good agreement between friction and chemical activity for the transition metals.

Metal Transfer

Figure 9 presents a surface replication electron micrograph of a wear track on the {111} diamond surface generated by a single-pass of sliding of a titanium rider at a load of 0.2 N across the surface. It is obvious from this photograph that a large amount of metal transfers to the diamond surface. The transferred titanium is a thin film which is streaky and parallel to the sliding direction.

Figure 10 presents an energy dispersive X-ray profile of an area which includes the small dark (black) debris shown in the center of figure 9. The profile shows titanium and copper peaks. The copper peaks in the spectrum are associated with the element of the specimen mesh-holder. The titanium peaks reveal the element of the black debris. Thus, in figure 9 the black debris is a part of a titanium film that transferred to the diamond surfaces and that was subsequently peeled off from the surface, while the replica of the specimen surface was being prepared.

All the metals shown in figures 6 and 8 transferred to the surfaces of nonmetals with sliding (refs. 1 to 4). These results indicate that (1) when metals and nonmetals are brought into contact, adhesion occurs, the interfacial bond is generally stronger than the cohesive bond in the cohesively weaker metal, and (2) on separation of the metal and nonmetal in sliding, fracture occurs generally in the metal.

The chemical affinity of metal to nonmetal plays an important role in the metal transfer and the form of metal wear debris generated by fracture of cohesive bond (ref. 2). In general the less active the metal, the less transfer to the nonmetal. Titanium having much stronger chemical affinity to the elements of the nonmetals exhibited the greatest amount of transfer.

Figure 11 presents a typical scanning electron micrograph of the rider wear scar on titanium resulting from a single pass of the titanium rider over the diamond {111} surface in vacuum. The wear scar on the metal rider revealed, generally, a large number of plastically deformed grooves, and is very similar to that on a metal rider after sliding against other nonmetals.

CONCLUSIONS

As a result of sliding friction experiments conducted with various transition metals in contact with nonmetallic hard materials, such as diamond, silicon carbide, boron nitride, and manganese-zinc ferrite, the following conclusions are drawn:

(1)   The coefficient of friction for nonmetals in contact with various metals is related to the relative chemical activity (d valence bond character) of those metals in ultra high vacuum. The more active the metal, the higher the coefficient of friction.

(2)   All the metals examined transferred to the surfaces of nonmetals in sliding. The more active the metal, the greater the transfer to nonmetals.

REFERENCES

1. K. Miyoshi and D. H. Buckley, Adhesion and Friction of Single-Crystal Diamond in Contact with Transition Metals, Appl. Surface Sci., 6: 161 (1980).

2. K. Miyoshi and D. H. Buckley, Friction and Wear Behavior of Single-Crystal Silicon Carbide in Sliding Contact with Various Metals, ASLE, Trans., 22: 245 (1979).

3. D. H. Buckley, Friction and Transfer Behavior of Pyrolytic Boron Nitride in Contact with Various Metals, ASLE, Trans., 21: 118 (1978).

4. K. Miyoshi and D. H. Buckley, Friction and Wear of Single-Crystal Manganese-Zinc Ferrite, Wear, 66: 157 (1981).

5. L. Pauling, A Resonating-Valence-Bond Theory of Metals and Intermetallic Compounds, Proc. R. Soc., London, A196: 343 (1949).

6. P. G. Lurie and J. M. Wilson, A Study of the Diamond Surface Using Electron Spectroscopy, Diamond Res., 26 (1976).

7. J. M. Thomas and L. L. Evans, Surface Chemistry of Diamond: A Review, Diamond Res., 2 (1975).

8. P. G. Lurie and J. M. Wilson, The Diamond Surface,

   I. The Structure of the Clean Surface

   and Interaction with Gases and Metals.

   Surface Sci. 65: 453 (1977).

9. A. J. Van Bommel, J. E. Crombeen, and A. Van Tooren, LEED and Auger Electron Observations of the SiC (0001) Surface, Surface Sci., 48: 463 (1975).

10. K. Miyoshi; and D. H. Buckley; Effect of Oxygen and Nitrogen Interactions on Friction of Single-Crystal Silicon Carbide, NASA TP - 1265 (1978)..

(d) After 45 minutes of argon-ion bombardment.

A_1 A_0
A_2
A_3
A_r

(e) After 60 minutes of argon-ion bombardment.

Electron energy, eV

(a) Before argon-ion bombardment.

(b) After 15 minutes of argon-ion bombardment.

dN(E)/dE

(c) After 30 minutes of argon-ion bombardment.
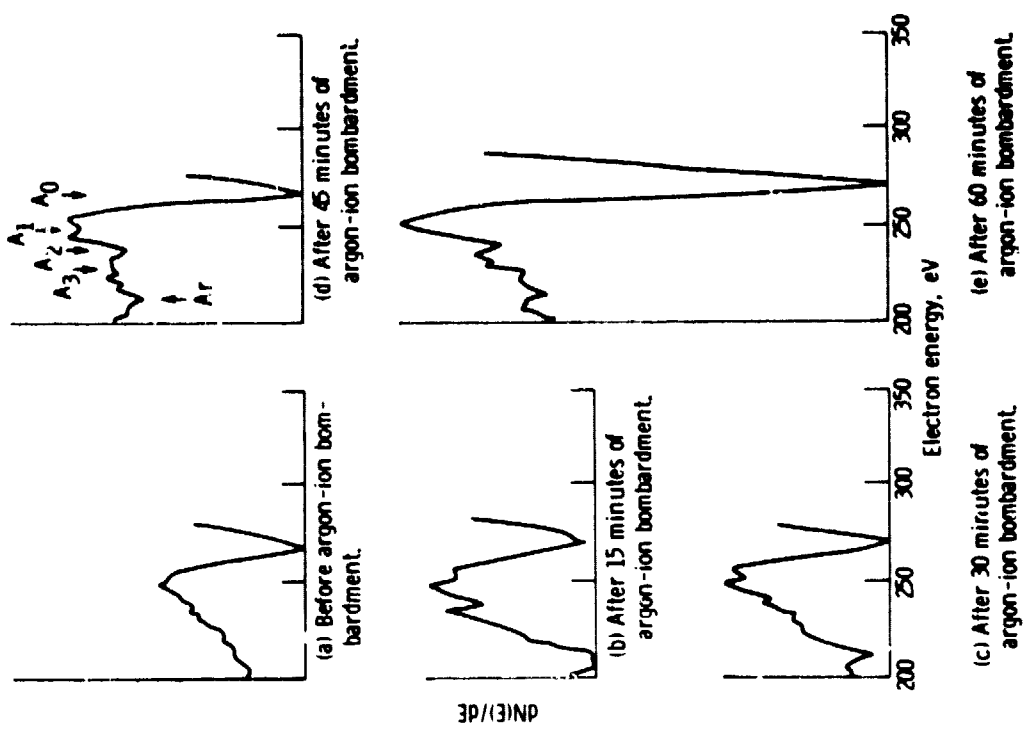
Figure 2. - Comparison of fine structure of the carbon Auger emission spectra for diamond.

Direction of sliding

Flat specimen

Hemispherical rider

Translational motion

Load

Adhesive force

Friction force

Gimbal
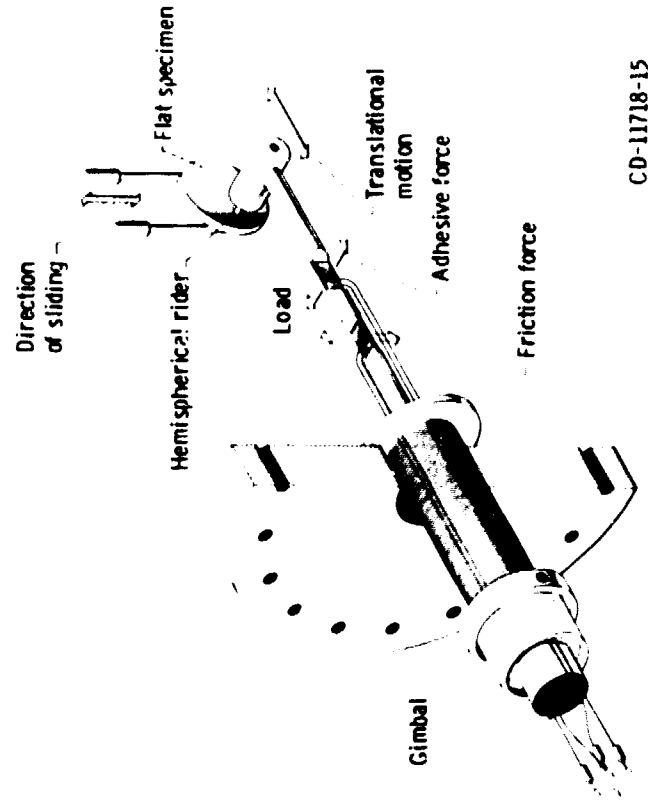
CD-11718-15

Figure 1. - Ultra high vacuum friction and wear apparatus.
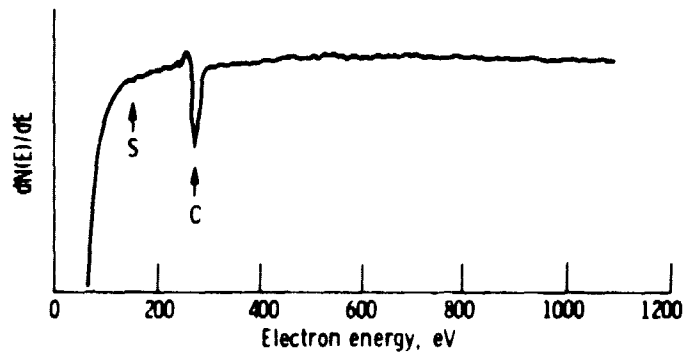
Figure 3. – Auger emission spectroscopy spectrum for diamond.

(a) Silicon carbide (0001) surface.

(b) Pyrolytic boron nitride (0001) surface.

Electron energy
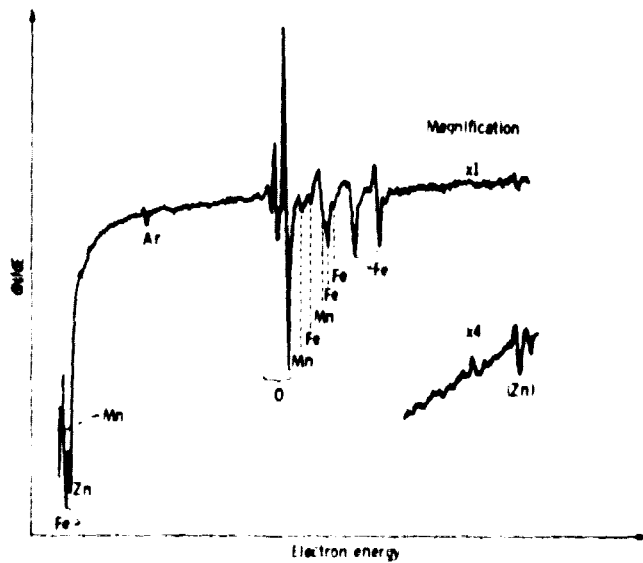
(c) Manganese-zinc ferrite (110) surface.

Figure 4. - Auger electron spectroscopy spectra for sputter cleaned nonmetals.
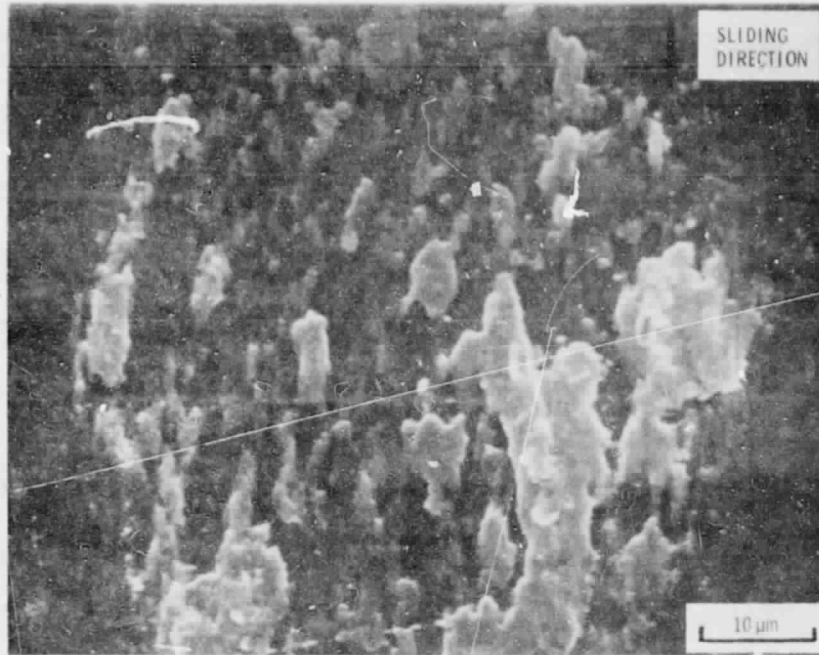
(a) TITANIUM TRANSFER AT COMMENCEMENT OF SLIDING.
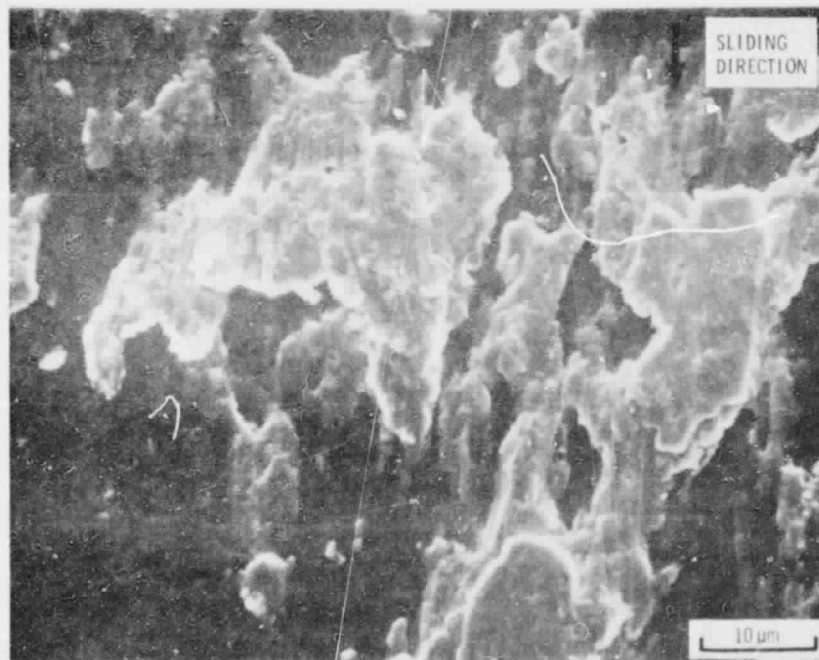
(b) TITANIUM TRANSFER DURING SLIDING.

Figure 5. - Titanium transferred to single-crystal silicon carbide as a result of single pass of rider in vacuum. Silicon carbide (0001) surface; sliding direction <1010>; sliding velocity, 3×10^{-3} m/min load, 0.3 N; room temperature; vacuum pressure, 10^{-8} Pa.

dN(E)/dE

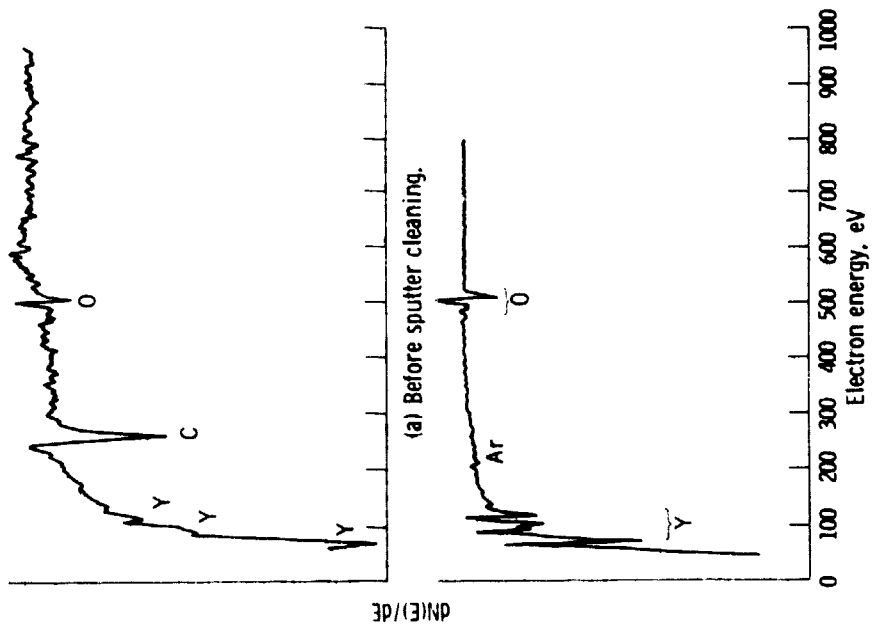(a) Before sputter cleaning.

(b) After sputter cleaning.

Electron energy, eV

Figure 7. - Auger emission spectroscopy spectrum for yttrium.

Coefficient of friction

Percent d character of metal bond

Figure 6. - Coefficient of friction as function of percent of metal d bond character for single-crystal diamond (111) surface in sliding contact with transition metals in vacuum. Sliding direction, $\langle 1\bar{1}0 \rangle$; sliding velocity, 3×10^{-3} m/min; load, 0.05 to 0.3 N; room temperature; vacuum pressure, 10^{-8} Pa.
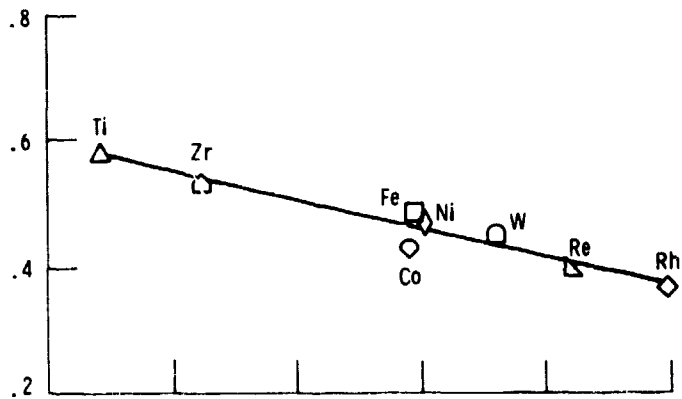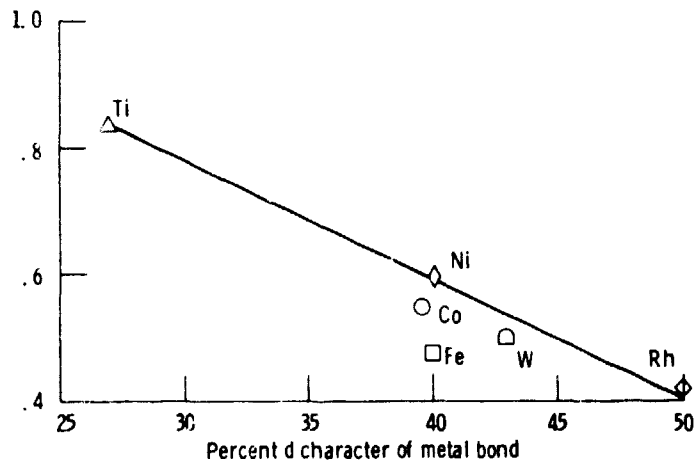
(a) Silicon carbide (0001) surface.
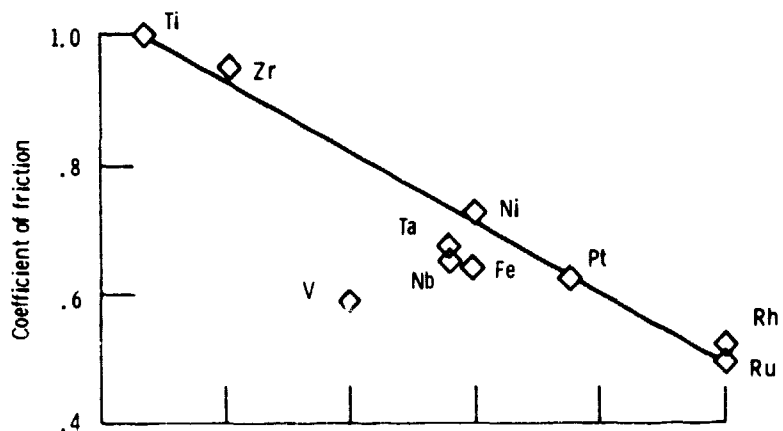
(b) Pyrolytic boron nitride (0001) surface.

(c) Manganese-zinc ferrite (110) surface.

Figure 3. - Coefficient of friction as function of percent of d bond character of various metals in sliding contact with nonmetals in vacuum. Single pass; sliding velocity, 3 or 0.7×10^{-3} m/min; load, 0.3 N; room temperature; vacuum pressure, 10^{-8} Pa.

Figure 9. - Replication electron micrograph of wear track on (111) diamond surface. Single pass of titanium rider; sliding direction, $\langle 1\bar{1}0 \rangle$; sliding velocity, 3×10^{-3} m/min; load, 0.2 N; room temperature; vacuum pressure, 10^{-8} Pa.
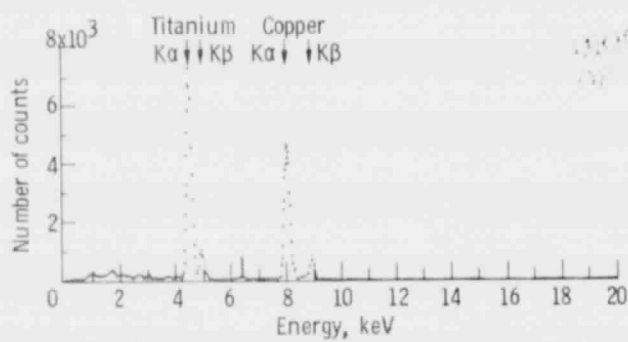
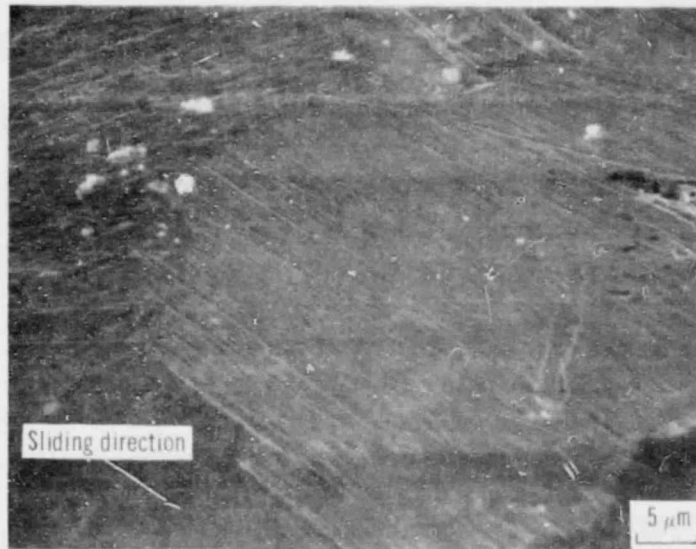Figure 10. - Energy dispersive X-ray profile of a piece of wear debris.

Figure 11. - Wear scar on titanium rider produced during sliding contact with diamond. Single pass on diamond {111} surface; sliding direction, ⟨110⟩ ; sliding velocity, 3×10^{-3} m/min; load, 0.2 N; sliding distance, 2.5×10^{-3} m; room temperature; vacuum pressure, 10^{-8} Pa.